HYBRID OPTIMISATION OF THz-DRIVEN TAPERED WAVEGUIDES FOR SYNCHRONOUS ACCELERATION OF WEAKLY RELATIVISTIC HIGH-QUALITY ELECTRON BUNCHES

F. Peczek*, [1], R. Appleby[1], J. Bradbury[1], G. Burt[2], D. Graham[1], M. Hibberd[1], S. Jamison[2], R. Letizia[2], L. Nix[2]
The Cockcroft Institute, Sci-Tech Daresbury, Daresbury, UK
[1]also at The University of Manchester, Manchester, UK
[2]also at Lancaster University, Lancaster, UK

Abstract

Downscaling particle accelerators is crucial to expanding their range of applications. Dielectric-lined waveguides (DLWs) can support hybrid modes with a strong accelerating component. Excited by terahertz (THz) frequency pulses, DLWs can deliver high accelerating gradients over cm-scale interaction lengths, promising the development of future compact electron accelerators. By precisely tailoring the waveguide geometry, the modal field profile and phase velocities can be tuned to maintain synchronisation between the weakly relativistic bunches and the accelerating mode over extended distances. Here, we design and evaluate THz-driven tapered DLWs delivering high-quality, MeV-level electron bunches in two types of symmetrical DLW waveguides: rectangular and cylindrical. We use analytic models of accelerating modes to simulate transport and acceleration of an externally injected 100-keV electron beam across various DLW geometries. A genetic algorithm is employed to identify Pareto-optimal geometries based on the final bunch characteristics.

INTRODUCTION

The key to more compact and affordable accelerators of the future is to push for higher accelerating gradients and enhanced beam quality. THz structures offer a promising solution that delivers exceptional control over the longitudinal and transverse phase space of sub-picosecond electron bunches. The gradients of $1\,\mathrm{GeV\,m^{-1}}$ have been demonstrated in THz-driven DLW waveguides [1].

Moreover, the last few decades have brought major advances in THz-generation technology, especially laser-driven sources, such as optical rectification in lithium niobate ($LiNbO_3$) [2–4]. To reach longer pulse lengths (satisfying narrowband requirement of accelerating structures), method was developed utilising, instead of a single crystal, stacks of periodically-poled lithium niobate (PPLN) wafers [5, 6].

In the subrelativistic regime, the particle velocity increases significantly throughout the interaction, and it quickly slips out of phase alignment in a constant-phase-velocity structure. Several schemes have been proposed to address this issue, including the use of phase shifters [7], multi-stage acceleration [8], and tapered geometry [9, 10]. By tailoring the cross-sectional geometry of the DLW along its longitudinal direction, the phase velocity of the accelerating waveform can be adjusted to maintain synchronism with the accelerated bunch. Tapered design, however, often requires a slowly varying geometry, which is challenging to manufacture. Here, we address this problem with a stepped geometry solution. We introduce a design process involving optimisation via a genetic algorithm that can be applied to a wide set of operating parameters, tolerance limits and desired bunch qualities.

* filip.peczek@manchester.ac.uk

TAPERED DIELECTRIC-LINED WAVEGUIDES

We consider two types of geometries offering distinctive accelerating modes: LSM_{11} in rectangular DLW and TM_{01} in cylindrical one. In the following, we describe their impact on beam dynamics depending on their transverse and longitudinal position.

Rectangular

Under the assumption that cross-sectional geometry determines the modal wavenumbers (k_x, k_y, k_z) through the dispersion relation and a lossless waveguide, the modal amplitude $A_R(z)$ can be found by considering the conservation of energy flux (power flow) [10]. Therefore, the accelerating LSM_{11} inside the vacuum region of a rectangular DLW, shown in Figure 1, takes form:

$$\begin{aligned}
E_x &= A_R(z) k_x k_{0y} \cos\left(k_x x + \frac{\pi}{2}\right) \cos\left(k_{0y} y\right), \\
E_y &= A_R(z) (k_x^2 + k_z^2) \sin\left(k_x x + \frac{\pi}{2}\right) \sin\left(k_{0y} y\right), \\
E_z &= A_R(z) k_z (-i k_{0y}) \sin\left(k_x x + \frac{\pi}{2}\right) \cos\left(k_{0y} y\right), \\
H_x &= -A_R(z) \omega \varepsilon_0 k_z \sin\left(k_x x + \frac{\pi}{2}\right) \sin\left(k_{0y} y\right), \\
H_y &= 0, \\
H_z &= A_R(z) i \omega \varepsilon_0 k_x \cos\left(k_x x + \frac{\pi}{2}\right) \sin\left(k_{0y} y\right),
\end{aligned} \tag{1}$$

where each term is multiplied by a travelling wave expression with a phase offset ϕ:

$$\exp\left(i\omega t - i\int_0^z k_z(z)\,dz + i\phi\right). \tag{2}$$

The accelerating mode LSM_{11} supported by the rectangular waveguide consists not only of a desired strong longitudinal electric field component but also non-zero transverse

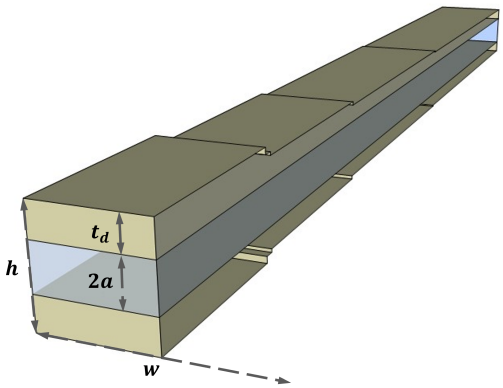

Figure 1: Section of stepped rectangular dielectric-lined waveguide (of width w, height h, and vacuum gap $2a$) lined with dielectric lining of thickness t_d embedded in conductive channel.

fields that impact bunch transverse dynamics. The transverse field distribution is determined by the multipole components of E_z, and E_x is dominated by E_y field in the subrelativistic regime. Hence, the transverse field is 0 at the central axis and $|E_x|$, and $|E_y|$ increase with $x \to \pm w/2$, and $y \to \pm a$ respectively. This has a profound impact on the beam as particles experience strong focusing in the y-axis and weak defocusing in the x-axis when behind the accelerating field crest, $\phi \in (\frac{1}{2}\pi, \pi)$, and accordingly strong defocusing in the y-axis and weak x-focusing when ahead of it, $\phi \in (\pi, \frac{3}{2}\pi)$.

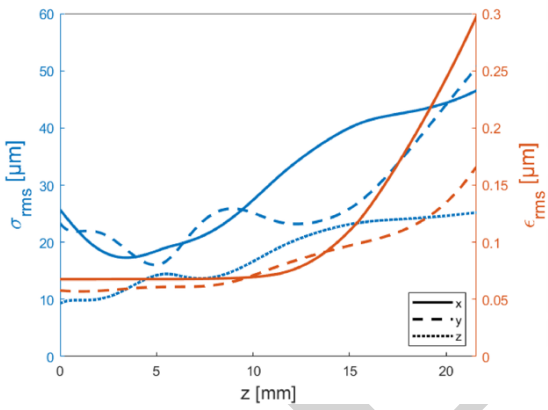

Figure 2: An example evolution of the bunch size and emittance over acceleration from 100 keV to 1 MeV in a tapered rectangular DLW structure.

Figure 2 clearly presents how in the rectangular structure focusing in x-direction correlates with y-direction defocusing and z-compression. Therefore, it is crucial that for a successful accelerating scheme, the phase velocity of the structure is chosen so the bunch can alternate between ahead and behind positions with respect to the accelerating crest.

Cylindrical

In the cylindrical structure, shown in Figure 3, under the assumption analogous to the rectangular, the cross-sectional geometry defines wavenumbers (k_r, k_ϕ, k_z) and the modal amplitude $A_C(z)$. These determine the field of TM_{01} which in the vacuum region can be expressed as:

$$\begin{aligned} E_z &= A_C(z) I_0(r k_r(z)), \\ E_r &= \frac{A_C(z) k_z(z)}{k_r(z)} I_1(r k_r(z)), \\ B_\phi &= \frac{A_C(z)\omega\epsilon_0\mu_0}{k_r(z)} I_1(r k_r(z)), \end{aligned} \tag{3}$$

where the radial propagation constant is expressed as $k_r = \sqrt{k_0^2 - k_z^2}$, and each term is multiplied by a travelling wave expression with phase offset ϕ:

$$\exp\left(i\omega t - i\int_0^z k_z(z)\,dz + i\phi\right). \tag{4}$$

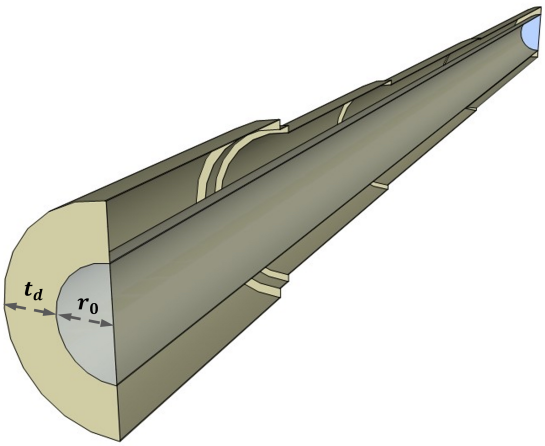

Figure 3: Section of stepped cylindrical dielectric-lined waveguide (with vacuum gap of radius r_0 and dielectric lining of thickness t_d) embedded in a conductive channel.

The radial dependence of the longitudinal field is closely related to the transverse fields defocusing the bunch. Ahead of the accelerating crest, $\phi \in (\pi, \frac{3}{2}\pi)$, the bunch experiences longitudinal focusing as the tail of the bunch experiences a higher field than its head. Within the same phase region, the transverse fields act on the bunch, resulting in transverse defocusing. Respectively, the bunch positioned behind the crest, $\phi \in (\frac{1}{2}\pi, \pi)$, experiences longitudinal defocusing and transverse focusing accordingly.

Figure 4 demonstrates how in cylindrical geometry, the radial focusing phase (behind the accelerating crest) corresponds to longitudinal decompression and, accordingly, the radial defocusing phase to longitudinal compression. Interestingly, staying in the transversely defocusing phase does not have a significant negative impact on the emittance.

DLW GEOMETRY OPTIMISATION

In this work, we keep the vacuum gaps (and width in the rectangular case) constant and taper the dielectric lining thickness of rectangular and cylindrical DLW to maximise

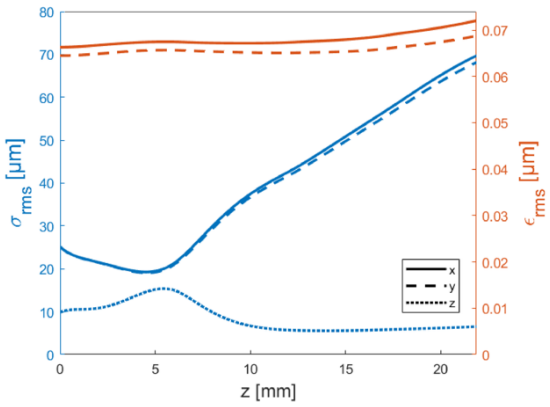

Figure 4: An example evolution of the bunch size and emittance over acceleration from 100 keV to 1 MeV in a tapered cylindrical DLW structure.

the longitudinal accelerating field while increasing the modal phase velocity. To simplify the geometry for manufacturability and reduce the parameter space, four segments of specific lengths and dielectric thicknesses are considered.

THz Excitation

As the group velocity of LSM_{11} and TM_{01} modes at subluminal phase velocity is significantly lower than the velocity of the 100 keV bunch, the accelerating DLW must be excited by a narrowband (multi-cycle) source to deliver a substantial interaction length within the structure. For the design simulations here, we consider a long, flat-topped pulse that can be feasibly generated in laser-driven PPLN sources. For our illustrative designs, 0.2 THz was chosen as the operating frequency, which corresponds to a 1.5 mm wavelength, considerably longer than the micrometre-scale bunches considered in this work. We consider excitation with up to 0.5 mJ of energy delivered as a narrowband 150 ps pulse of constant time-averaged power of 3.6 MW.

Genetic Algorithm Optimiser

To find a tapered geometry consisting of 4 segments of consecutively decreasing thickness of dielectric, a multi-objective genetic algorithm (MOGA) was used. The MOGA (NSGA-II MATLAB default [11]) has been implemented by wrapping it around a custom analytic field particle tracker (developed in MATLAB), utilising 4th order Runge-Kutta method and analytic fields derived in each segment. The number of optimisation objectives was constructed based on accelerated bunch qualities such as final energy E, energy spread ΔE_{RMS}, capture rate CR (defining the fraction of particles constituting the final bunch), and normalised projected transverse emittance ϵ_{xy}.

The result of optimisation of both geometry types is shown in Figure 5 where solutions are mapped according to their final qualities. In the case of rectangular geometry, higher final energies tend to correspond to lower capture rates and higher transverse emittances. The cylindrical geometries result in bunches of significantly lower transverse emittance

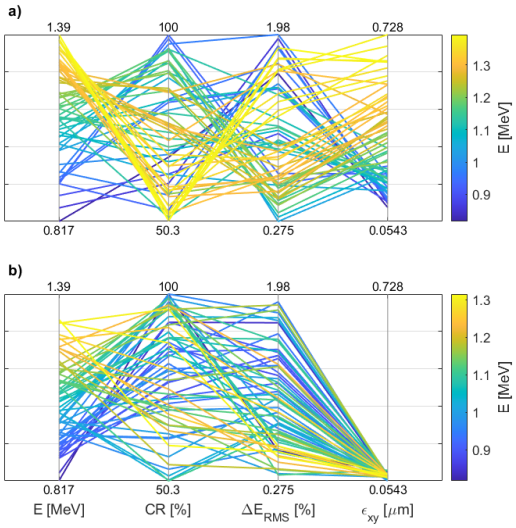

Figure 5: Rectangular a) and cylindrical b) DLW plot of final MOGA objective space for CR exceeding 50 % and ΔE_{RMS} below 2 %. Each line represents a solution characterised by four bunch qualities. The capture rate, CR, is defined as in [9].

than the rectangular ones. This can be attributed to the higher linearity of the radial fields with respect to transverse coordinates.

CONCLUSION

In this work, the MeV-level acceleration of a 100 keV electron bunch in THz-driven tapered DLW was demonstrated for both types of geometries. Simulations indicate that low-emittance 0.5 fC bunches can be accelerated from 100 keV to over 1 MeV in a 20-mm-structure with 0.5 mJ of energy in a multi-cycle 0.2 THz pulse. The advantage of our design method choice is its geometric robustness, which falls well within modern manufacturing capabilities, and the insight into the trade-off between the qualities of the final bunch. The presented designs showcase a potential for tabletop structures providing MeV-energy electron beams for ultrafast science experiments or subsequent synchronous accelerating stages.

REFERENCES

[1] B. D. O'Shea *et al.*, "Observation of acceleration and deceleration in gigaelectron-volt-per-metre gradient dielectric wakefield accelerators", *Nat. Commun.*, vol. 7, no. 1, p. 12763, Sep. 2016. doi:10.1038/ncomms12763

[2] T. I. Oh, Y. J. Yoo, Y. S. You, and K. Y. Kim, "Generation of strong terahertz fields exceeding 8 mv/cm at 1 khz and real-time beam profiling", *Appl. Phys. Lett.*, vol. 105, no. 4, p. 041103, Jul. 2014. doi:10.1063/1.4891678

[3] M. J. Cliffe, D. M. Graham, and S. P. Jamison, "Longitudinally polarized single-cycle terahertz pulses generated with high electric field strengths", *Appl. Phys. Lett.*, vol. 108, no. 22, p. 221102, May 2016. doi:10.1063/1.4953024

[4] J. A. Fülöp, S. Tzortzakis, and T. Kampfrath, "Laser-driven strong-field terahertz sources", *Advanced Optical Materials*, vol. 8, no. 3, p. 1900681, 2020. doi:10.1002/adom.201900681

[5] F. Lemery *et al.*, "Highly scalable multicycle thz production with a homemade periodically poled macrocrystal", *Commun. Phys.*, vol. 3, no. 1, p. 150, 2020. doi:10.1038/s42005-020-00421-2

[6] C. D. W. Mosley *et al.*, "Large-area periodically-poled lithium niobate wafer stacks optimized for high-energy narrowband terahertz generation", *Opt. Express*, vol. 31, no. 3, pp. 4041–4054, Jan. 2023. doi:10.1364/OE.475604

[7] D. Zhang, Y. Zeng, M. Fakhari, X. He, N. H. Matlis, and F. X. Kärtner, "Long range terahertz driven electron acceleration using phase shifters", *Appl. Phys. Rev.*, vol. 9, no. 3, p. 031407, Sep. 2022. doi:10.1063/5.0096685

[8] D. Zhang, M. Fakhari, H. Cankaya, A.-L. Calendron, N. H. Matlis, and F. X. Kärtner, "Cascaded multicycle terahertz-driven ultrafast electron acceleration and manipulation", *Phys. Rev. X*, vol. 10, no. 1, p. 011067, Mar. 2020. doi:10.1103/PhysRevX.10.011067

[9] L. J. R. Nix *et al.*, "Terahertz-driven acceleration of subrelativistic electron beams using tapered rectangular dielectric-lined waveguides", *Phys. Rev. Accel. Beams*, vol. 27, no. 4, p. 041302, Apr. 2024. doi:10.1103/PhysRevAccelBeams.27.041302

[10] F. Lemery, K. Floettmann, P. Piot, F. X. Kartner, and R. Aßmann, "Synchronous acceleration with tapered dielectric-lined waveguides", *Phys. Rev. Accel. Beams*, vol. 21, no. 5, p. 051302, May 2018. doi:10.1103/PhysRevAccelBeams.21.051302

[11] K. Deb, A. Pratap, S. Agarwal, and T. Meyarivan, "A fast and elitist multiobjective genetic algorithm: NSGA-II", *IEEE Trans. Evol. Comput.*, vol. 6, no. 2, pp. 182–197, 2002. doi:10.1109/4235.996017